

Remodeling of tick cytoskeleton in response to infection with *Anaplasma phagocytophilum*

Alejandro Cabezas-Cruz^{1,2}, Pilar Alberdi³, James J. Valdes^{1,4}, Margarita Villar³, Jose de la Fuente^{3,5}

¹Institute of Parasitology, Biology Center, Czech Academy of Sciences, 37005 Ceske Budejovice, Czech Republic, ²Faculty of Science, University of South Bohemia, Ceske Budejovice, Czech Republic, ³SaBio Instituto de Investigacion en Recursos Cinegeticos IREC (CSIC-UCLM-JCCM), 13005 Ciudad Real, Spain, ⁴Department of Virology, Veterinary Research Institute, Hudcova 70, CZ-62100 Brno, Czech Republic, ⁵Department of Veterinary Pathobiology, Center for Veterinary Health Sciences, Oklahoma State University, Stillwater, OK 74078 USA

TABLE OF CONTENTS

1. Abstract
2. Introduction
3. Materials and methods
 - 3.1. Annotation of the cytoskeleton components in the *I. scapularis* genome
 - 3.2. Characterization of the *I. scapularis* mRNA and protein levels in response to *A. phagocytophilum* infection
 - 3.3. Phylogenetic analysis of *I. scapularis* septins
 - 3.4. Immunofluorescence assay in *I. scapularis* midguts and salivary glands
 - 3.5. RNA interference in cultured ISE6 tick cells
 - 3.6. Analysis of tick cell mRNA levels by real-time RT-PCR
4. Results
 - 4.1. Cytoskeleton components identified in other organisms are present in the *I. scapularis* genome
 - 4.2. Classification of the *I. scapularis* septins
 - 4.3. The mRNA and protein levels of *I. scapularis* cytoskeleton components vary in response to *A. phagocytophilum* infection in a tissue-specific manner
 - 4.4. Functional studies support a role for cytoskeleton remodeling during *A. phagocytophilum* infection of tick cells
5. Discussion
6. Acknowledgements
7. References

1. ABSTRACT

The obligate intracellular pathogen *Anaplasma phagocytophilum* infects vertebrate and tick hosts. In this study, a genome-wide search for cytoskeleton components was performed in the tick vector, *Ixodes scapularis*. The available transcriptomics and proteomics data was then used to characterize the mRNA and protein levels of *I. scapularis* cytoskeleton components in response to *A. phagocytophilum* infection. The results showed that cytoskeleton components described in other model organisms were present in the *I. scapularis* genome. One type of intermediate filaments (laminin), a family of septins that was recently implicated in the cellular response to intracellular pathogens, and several members of motor proteins (kinesins and dyneins) that could be implicated in the cytoplasmic movements of *A. phagocytophilum* were found. The results showed that

levels of tubulin, actin, septin, actin-related proteins and motor proteins were affected by *A. phagocytophilum*, probably to facilitate infection in *I. scapularis*. Functional studies demonstrated a role for selected cytoskeleton components in pathogen infection. These results provided a more comprehensive view of the cytoskeletal components involved in the response to *A. phagocytophilum* infection in ticks.

2. INTRODUCTION

Ticks are blood feeding arthropod ectoparasites that transmit pathogens causing diseases in humans and animals worldwide (1). Among these pathogens, *Anaplasma phagocytophilum* (Rickettsiales: Anaplasmataceae) is an obligate

intracellular bacterium mainly transmitted by *Ixodes* spp. ticks in the United States, Europe, Africa and Asia (1–3). Diseases caused by *A. phagocytophilum* include human granulocytic anaplasmosis (HGA), equine and canine granulocytic anaplasmosis and tick-borne fever (TBF) of ruminants (1–3).

A. phagocytophilum infects vertebrate host granulocytes, and tick midgut, hemocytes and salivary glands (2–4). The development of *A. phagocytophilum* is complex and coordinated with the tick feeding cycle. Infection and colonization of ticks occurs first in midgut cells and then subsequently in other tissues including the salivary glands from where transmission occurs during feeding (3). To establish infection, *A. phagocytophilum* induce complex changes in tick and vertebrate host cells mediated by different mechanisms (4). These mechanisms appear to be common to ticks and vertebrate hosts, and include but are not limited to remodeling of the cytoskeleton, inhibition of cell apoptosis, manipulation of the immune response, and modification of cell epigenetics and metabolism (4).

During infection, *A. phagocytophilum* induce cytoskeleton remodeling through actin reorganization or spectrin differential regulation in both vertebrate host and ticks (5, 6). These results suggested that *A. phagocytophilum* induce cytoskeleton remodeling for infection and multiplication in tick cells. However, the mechanisms used by *A. phagocytophilum* for remodeling of tick cytoskeleton have not been fully characterized.

To better characterize the mechanisms used by *A. phagocytophilum* to remodel cytoskeleton during infection of tick cells, the dynamics of the cytoskeleton was characterized in the tick vector, *I. scapularis* in response to pathogen infection. First, the composition of tick cytoskeleton was annotated using the recently published genome of *I. scapularis* (7). Then, previously published transcriptomics and proteomics data (8, 9) was used to characterize the mRNA and protein levels of cytoskeleton components in response to *A. phagocytophilum* infection of *I. scapularis* nymphs, female midguts and salivary glands, and ISE6 cultured tick cells. Finally, functional studies were conducted in ISE6 tick cells to provide additional support for the role of these molecules during pathogen infection. These results expanded our knowledge of the dynamics of tick cytoskeleton during *A. phagocytophilum* infection.

3. MATERIALS AND METHODS

3.1. Annotation of the cytoskeleton components in the *I. scapularis* genome

The *I. scapularis* genome (7) was searched with the specific names of genes encoding for cytoskeleton components. When records were not obtained using specific enzyme names, then the *I.*

scapularis genome was searched with the Blastp tool from the Basic Local Alignment Search Tool (BLAST) using the human orthologs as 'query' (10, 11). The sequences with the lowest E-value were selected. The conserved domains of identified protein sequences were classified using the protein families database Pfam (12). The *I. scapularis* orthologs found in the tick genome were double-checked by searching the *Homo sapiens* genome database using as queries the tick homologs identified in the previous step.

3.2. Characterization of the *I. scapularis* mRNA and protein levels in response to *A. phagocytophilum* infection

The quantitative transcriptomics and proteomics data for uninfected and *A. phagocytophilum*-infected *I. scapularis* nymphs, female midguts and salivary glands, and ISE6 cultured cells were obtained from previously published results (8, 9) and deposited at the Dryad repository database, NCBI's Gene Expression Omnibus database and ProteomeXchange Consortium via the PRIDE partner repository with the dataset identifier PXD002181 and doi: 10.6019/PXD002181. The identified genes encoding for cytoskeleton components were searched against the transcriptomics and proteomics data to characterize their mRNA and protein levels in response to *A. phagocytophilum* infection.

3.3. Phylogenetic analysis of *I. scapularis* septins

To genetically characterize the *I. scapularis* septins, a phylogenetic analysis was conducted using sequences from mammals (*H. sapiens* and *Mus musculus*), insects (*Anopheles gambiae* and *Drosophila melanogaster*) and chelicerates (*Limulus polyphemus*, *Stegodyphus mimosarum* and *Metaseiulus occidentalis*) (Figure 1). The sequences were aligned with the Multiple Alignment using Fast Fourier Transform program (MAFFT, version 7) configured for the highest accuracy (13, 14). Non-aligned regions were removed with Gblocks (version 0.9.1b) (15). The evolutionary history was inferred by using the Maximum Likelihood method based on the JTT matrix-based model implemented in Molecular Evolutionary Genetics Analysis (MEGA, version 6) software (16, 17). Reliability of internal branches was assessed using the bootstrapping method (1000 bootstrap replicates). Graphical representation and editing of the phylogenetic tree was performed with MEGA6.

3.4. Immunofluorescence assay in *I. scapularis* midguts and salivary glands

Female ticks fed on *A. phagocytophilum*-infected and uninfected sheep and fixed with 4% paraformaldehyde in 0.2 M sodium cacodylate buffer were embedded in paraffin and used to prepare sections

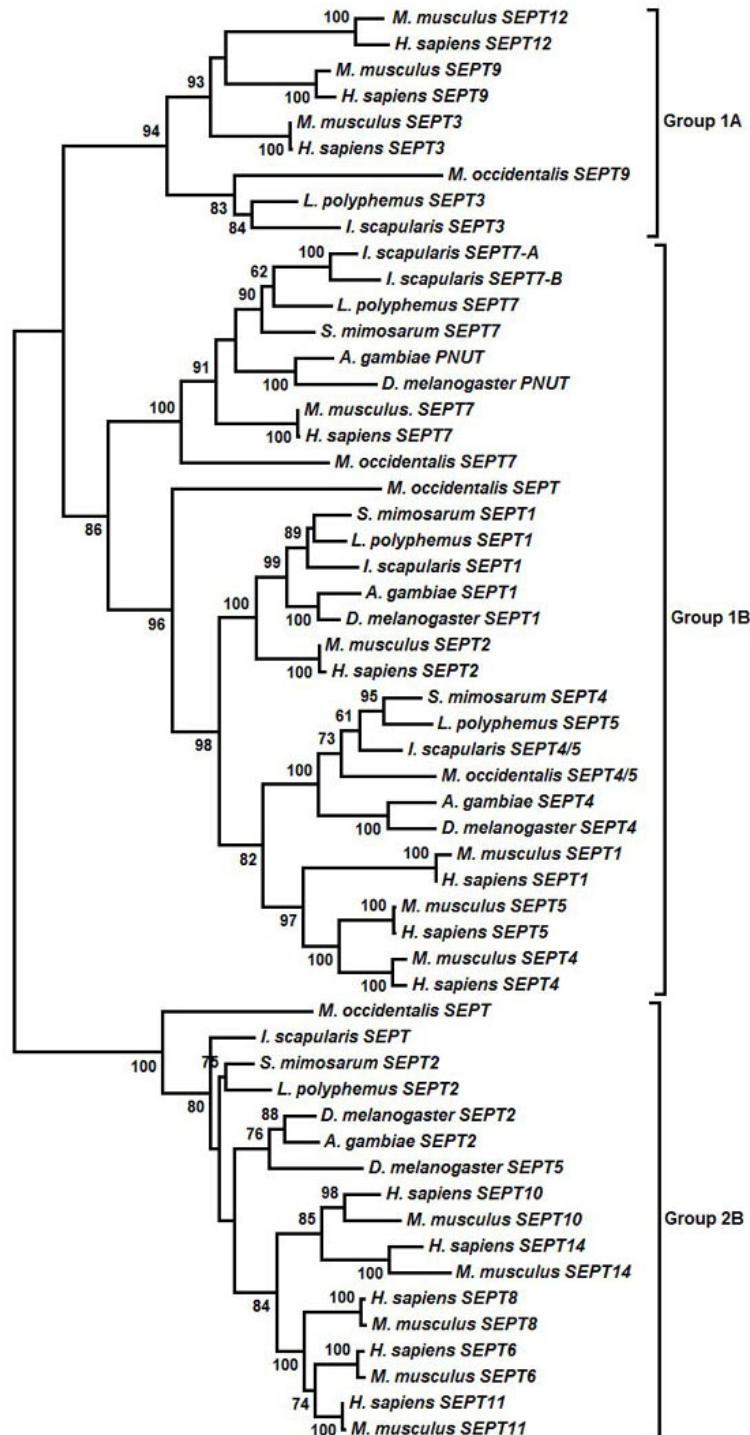


Figure 1. Classification of *I. scapularis* septins. A maximum likelihood phylogenetic tree was built using the amino acid sequences of the septins identified in *I. scapularis* and their orthologs (names of the orthologs and accession numbers are shown in parenthesis): *I. scapularis* (SEPT Group 2B, EEC07992; SEPT1, EEC12890; SEPT3, EEC02884; SEPT4/5, EEC07178; SEPT7A, EEC06789 and SEPT7B, EEC07929); *H. sapiens* (SEPT1, NP_443070; SEPT2, AAH14455; SEPT3, AAG00517; SEPT4, AAH18056; SEPT5, AAH25261; SEPT6, AAN76547; SEPT7, AAH93640; SEPT8, NP_001092281; SEPT9, AAH21192; SEPT10, AAF67469; SEPT11, AAH63615; SEPT12, AAH35619 and SEPT14, NP_997249), *M. musculus* (SEPT1, NP_059489; SEPT2, NP_035021; SEPT3, XP_006521054; SEPT4, XP_006532561; SEPT5, AAH45333; SEPT6, NP_064326; SEPT7, NP_033989; SEPT8, XP_011247135; SEPT9, XP_006533807; SEPT10, XP_011241558; SEPT11, NP_001009818; SEPT12, XP_006522641 and SEPT14, Q9DA97), *A. gambiae* (SEPT1, XP_312282; SEPT2, XP_309977; SEPT4, XP_311306 and PNUT, XP_308277), *D. melanogaster* (SEPT1, NP_523430; SEPT2, NP_524417; SEPT4, NP_728003; SEPT5, NP_651961 and PNUT, P40797), *L. polyphemus* (SEPT1, XP_013780505; SEPT2, XP_013779075; SEPT3, XP_013794450; SEPT5, XP_013777903 and SEPT7, XP_013775108;), *S. mimosarum* (SEPT1, KFM60685; SEPT2, KFM59146; SEPT4, KFM75885 and SEPT7, KFM73665) and *M. occidentalis* (SEPT Group 2B, XP_003748058; SEPT, XP_003738244; SEPT, XP_003748409; SEPT7 and XP_003743448; SEPT9, XP_003744811). Bootstrap values (1000 bootstrap replicates) for internal branches are shown.

Table 1. Sequences of siRNAs and oligonucleotide primers for real-time RT-PCR of tick transcripts

Target	GenBank accession No.	Sense sequence 5'-3'
tropomyosin siRNA1	ISCW008202	AAAGAGAAGUACAAAGCUAUU
tropomyosin siRNA2	ISCW008202	AGGAGAAAGAGAAGUACAAU
Control Rs86 siRNA	DQ201646	CGGUAAAUGUCGAAGCAAU
Tropomyosin PCR	ISCW008202	GAGCCGAGTTTGCCGAGAG ACTTGGTAGCGGTAGAAACGG
ribosomal protein S4 (rps4) PCR	DQ066214	GGTGAAGAAGATTGTCAAGCAGAG TGAAGCCAGCAGGGTAGTTTG

on glass slides as previously described (8). The paraffin was removed from the sections through two washes in xylene and the sections were hydrated by successive 5 min washes with a graded series of 100%, 96% and 65% ethanol and finally with distilled water. Next, the slides were treated with Proteinase K (Dako, Barcelona, Spain) for 7 min, washed with 0.1% PBS-Tween 20 (Sigma-Aldrich, St. Louis, MI, USA) and blocked with 2% bovine serum albumin (BSA; Sigma-Aldrich) in PBS-Tween 20 during 1h at room temperature. The slides were then incubated overnight at 4°C with rat anti-tropomyosin monoclonal antibodies (ab50567; Abcam, Cambridge, UK) diluted 1:100 in 2% BSA/PBS-Tween 20. Preimmune serum was used as control. After 3 washes with PBS-Tween 20, the slides were incubated for 1h with rabbit anti-mouse IgG, which also recognize rat monoclonal antibodies, conjugated with FITC (Sigma-Aldrich) diluted 1:160 in 2% BSA/PBS-Tween 20. Finally, after two washes with PBS the slides were mounted on ProLong Diamond Antifade Mountant with DAPI reagent (Thermo Scientific™, Madrid, Spain). The sections were examined using a Zeiss LSM 800 with Airyscan (Carl Zeiss, Oberkochen, Germany).

3.5. RNA interference in cultured ISE6 tick cells

The *I. scapularis* embryo-derived cell line ISE6 (provided by U.G. Munderloh, University of Minnesota, USA) was maintained in L-15B300 medium as described previously (18). Tick cells were cultured in sealed containers in ambient air at 31°C and inoculated with the *A. phagocytophilum* human isolate NY18 (19, 20). Small interfering RNAs (siRNAs) homologous to *I. scapularis* tropomyosin gene (ISCW008202) were synthesized by GE Healthcare Dharmacon Inc. (Lafayette, CO, USA) (Table 1). The unrelated siRNA Rs86 (DQ201646) was used as negative control (Table 1). RNAi experiments were conducted in cell cultures by incubating tick cells with 100 nM of each siRNA in 24-well plates, using 6 wells per treatment. Control cells were incubated with the unrelated control Rs86 siRNA. After 48 h of siRNA exposure, tick cells were inoculated with 500 ul/well of cell-free *A. phagocytophilum* human NY18 isolate semi-purified from approximately 5×10^6 infected tick cells (60% infected cells). Briefly, tick cells were mechanically disrupted with a syringe and a 27 gauge

needle, centrifuged at $200 \times g$ for 5 min to remove cells debris and intact cells and the volume adjusted to 12 ml with L-15B300 culture medium then 500 ul was added per well or they were mock infected by adding 500 ul/well of culture medium alone. Cells were incubated for an additional 72 h, collected, and processed for DNA and RNA extraction. Total RNA was used to analyze tropomyosin gene knockdown by real-time RT-PCR with respect to the Rs86 control. DNA was used to quantify the *A. phagocytophilum* levels by *msp4* PCR as described previously (6). *A. phagocytophilum* DNA levels were compared between treated and control cells by Student's t-test with unequal variance between test and control siRNA treated cells ($P=0.05$; $N=6$ biological replicates).

3.6. Analysis of tick cell mRNA levels by real-time RT-PCR

Total RNA was extracted from uninfected and *A. phagocytophilum*-infected ISE6 cells using TriReagent (Sigma, St. Louis, MO, USA) following the manufacturer's recommendations. Real-time RT-PCR was performed on RNA samples with gene-specific primers (Table 1) at 55°C using the iScript One-Step RT-PCR Kit with SYBR Green and the iQ5 thermal cycler (Bio-Rad, Hercules, CA, USA) following the manufacturer's recommendations. A dissociation curve was run at the end of the reaction to ensure that only one amplicon was formed and that the amplicons denatured consistently in the same temperature range for every sample (21). The mRNA levels were normalized against ribosomal protein S4 (*rps4*; 22) using the genNorm method (ddCT method as implemented by Bio-Rad iQ5 Standard Edition, Version 2.0.) (23). The results were compared by Student's t-test with unequal variance between test and control siRNA treated cells ($P=0.05$; $N=6$ biological replicates).

4. RESULTS

4.1. Cytoskeleton components identified in other organisms are present in the *I. scapularis* genome

The eukaryotic cytoskeleton is composed of three major protein superfamilies, actin, tubulin, and

intermediate filaments (IFs) (24). However, recently septins have been regarded as the fourth component of the cytoskeleton (25). Actin and tubulin form dynamic actin filaments and microtubules, respectively. Around 50 different types of specialized proteins that form more static filaments compose the filamentous structures of the IFs (26). The proteins forming the IFs have been grouped into six groups (Types I-VI) based on similarities between their amino acid sequences. These groups include acidic and neutral keratins (Types I and II, respectively), vimentin, desmin, glial fibrillary acidic protein and peripherin (Type III), neurofilament (NF) proteins NF-L, NF-M and NF-H and α -Internexin (Type IV), nuclear lamins (Type V), and nestin (Type VI) (26). Most types of IFs are cytoplasmic, but lamins are localized in the cell nucleus (26). Septins are GTP-binding proteins that form hetero-oligomeric complexes and higher-order structures, which play important roles as scaffolds for protein recruitment as well as diffusion barriers for subcellular compartmentalization, notably during host-microorganism interactions (25). Septins have been found in both unicellular and multicellular organisms (27).

In addition to Types I-VI IF basic components, there are other proteins that regulate or interact with them and give full functionality to the cytoskeleton. Among these proteins are the tropomodulins (Tmods), leiomodins (Lmods), tropomyosins, profilins, formins, and actin-depolymerizing factors (ADFs) (24). The Tmod family includes four Tmods and three Lmods in humans. Tmods cap the pointed ends of actin filaments in actin cytoskeleton structures in a developmentally regulated and tissue-specific manner (28). Tropomyosins are actin-binding proteins that constitute core components of the microfilament and regulate actin dynamics (29). Profilins are ubiquitous actin-monomer binding proteins that regulate microfilament polymerization (30). Formins are a family of proteins that govern different aspects of cellular physiology by remodeling actin and microtubules (31). Finally, ADFs depolymerize actin filaments and are modulators of actin filament dynamics and other cellular processes, from signal transduction to the cytonuclear trafficking of actin (32).

The major cytoskeleton components found in other organisms were identified in the *I. scapularis* genome (Table 2). In agreement with previous reports that arthropods do not have most cytoplasmic IFs (33), we did not identify IFs Types I, II, III, IV and VI in the genome of *I. scapularis*. However, two nuclear lamins, members of Type V IFs were identified (Table 2). Additionally, 6 septins, 7 actins and 16 tubulins, including 7 α -tubulins, 6 β -tubulins, 1 γ -tubulin, 1 ϵ -tubulin, and 1 δ -tubulin were also identified (Table 2). Of the 6 families of actin-related proteins analyzed (ADF, Tmod, Lmod, Tm, profiling and formin), only Lmod was not identified in the

genome of *I. scapularis* (Table 1). Comparatively, the molecular components identified in the *I. scapularis* cytoskeleton are found in other organisms such as *H. sapiens*, *D. melanogaster* and *Saccharomyces cerevisiae* (Table 3). However, more tubulins were found in *I. scapularis* when compared to *D. melanogaster* and *S. cerevisiae* (Table 3). For motor proteins, 10 kinesins and 20 dyneins were identified in the *I. scapularis* genome (Table 4).

4.2. Classification of the *I. scapularis* septins

Because of the importance of septins in the molecular interactions between hosts and microorganisms (25), the *I. scapularis* septins were characterized in more detail using a phylogenetic analysis (Figure 1). The number of septins varies between different organisms. For example, humans have 13 septins (SEPT1-SEPT12 and SEPT14; SEPT13 is a pseudogene now called SEPT7p2), *S. cerevisiae* have 7 septins (SceCdc3, SceCdc10, SceCdc11, SceCdc12, SceShs1, SceSpr28, SceSpr3), and *D. melanogaster* have 5 septins (DmePnut, DmeSep1, DmeSep2, DmeSep4 and DmeSep5) (25, 27, 34) (Table 3). Based on the phylogenetic analysis, animal septins were classified into groups 1A, 1B and 2B (27). Six septins were identified in *I. scapularis* (Tables 2 and 3), and were represented in the three groups of animal septins (Figure 1). Using amino acid sequences, four *I. scapularis* septins were classified unambiguously as SEPT1, SEPT3, and two copies of SEPT7 (A and B) (Figure 1). The clustering of the other two *I. scapularis* septins did not allow for a definitive classification. One septin clustered as SEPT4/5, and the other clustered within Group 2B, but without a clear phylogenetic relationship to any particular septin family member (Figure 1). Another classification grouped human septins into four groups named as SEPT2 (including SEPT1, SEPT2, SEPT4 and SEPT5), SEPT3 (including SEPT3, SEPT9 and SEPT12), SEPT6 (including SEPT6, SEPT8, SEPT10, SEPT11 and SEPT14), and SEPT7 (including SEPT7 only) (25). Based on this classification, *I. scapularis* septins were represented only in groups SEPT2, SEPT3 and SEPT7.

4.3. The mRNA and protein levels of *I. scapularis* cytoskeleton components vary in response to *A. phagocytophilum* infection in a tissue-specific manner

The finding of the genes encoding major eukaryotic cytoskeleton components in *I. scapularis* suggested the existence of an evolutionarily conserved cytoskeleton in ticks that have not been fully characterized. The tick response to *A. phagocytophilum* infection is largely regulated at the transcriptional level (8, 9, 35). Furthermore, the existence of histones and histone modifying

Table 2. Annotation of cytoskeleton components in the *I. scapularis* genome

Protein family/subunit	Genome accession	GenBank ID	Length (amino acids)
Tubulins			
α -tubulin	ISCW017473	EEC02794	634
α -tubulin	ISCW000908	EEC01375	386
α -tubulin	ISCW015260	EEC20578	451
α -tubulin	ISCW003527	EEC05915	451
α -tubulin	ISCW004211	EEC05710	499
α -tubulin	ISCW015258	EEC20577	394
α -tubulin	ISCW009719	EEC12427	203
β -tubulin	ISCW017136	EEC03517	446
β -tubulin	ISCW017133	EEC03514	446
β -tubulin	ISCW018899	EEC08136	271
β -tubulin	ISCW021482	EEC14639	456
β -tubulin	ISCW005137	EEC06076	300
β -tubulin	ISCW024581	EEC11984	239
γ -tubulin	ISCW023762	EEC19090	137
ϵ -tubulin	ISCW002714	EEC02931	465
δ -tubulin	ISCW022899	EEC16789	451
Actins			
Actin	ISCW024111	EEC03934	335
Actin	ISCW000900	EEC02017	387
Actin	ISCW022367	EEC17923	262
Actin	ISCW012075	EEC17528	296
Actin	ISCW009848	EEC12237	258
Actin	ISCW022123	EEC16870	376
Actin	ISCW016175	EEC00680	374
Septins			
Septin (Group 2B)	ISCW018518	EEC07992	426
Septin 1	ISCW020030	EEC12890	326
Septin 3	ISCW002975	EEC02884	250
Septin 7B	ISCW006074	EEC07929	424
Septin 4/5	ISCW018707	EEC07178	365
Septin 7A	ISCW018169	EEC06789	418
Intermediate filaments (IFs) - Lamins			
Lamin	ISCW000339	EEC00876	579
Nuclear lamin	ISCW016974	EEC02727	436
Actin-related proteins			
Formins			
Formin	ISCW016448	EEC01812	685
Formin	ISCW003576	EEC05276	75
Formin	ISCW006839	EEC09040	148
Formin	ISCW015518	EEC20216	153
Profilins			
Profilin	ISCW023148	EEC18404	130

Tropomodulins			
Tropomodulin	ISCW005954	EEC07356	132
Tropomyosins			
Tropomyosin	ISCW008202	EEC09701	306
Tropomyosin	ISCW019008	EEC08102	582
Tropomyosin	ISCW009063	EEC11956	39
Tropomyosin	ISCW006460	EEC07740	396
Tropomyosin	ISCW003781	EEC06213	362
Actin-depolymerizing factors			
Actin-depolymerizing factor	ISCW006326	EEC07958	147

Table 3. Number of cytoskeleton components in *I. scapularis* and other species

Species	Actin	Tubulin	Septins	ADF	Tmod	Lmod	Tm	Profilin	Formin
<i>I. scapularis</i>	7	16	6	1	1	0	5	1	4
<i>H. sapiens</i>	6	24	13	3	4	3	4	3	13
<i>D. melanogaster</i>	8	7	5	1	0	0	2	1	5
<i>S. cerevisiae</i>	1	4	7	1	0	0	2	1	2

Data on the number of all proteins, except septins, in *H. sapiens*, *D. melanogaster* and *S. cerevisiae* were collected from Gunning *et al.* (2015). Data on the number of septins were collected from Mostowy and Cossart (2012) for *H. sapiens* and *S. cerevisiae*, and from Adam *et al.* (2000) for *D. melanogaster*. Abbreviations: ADF, actin-depolymerizing factor; Tmod, tropomodulin; Lmod, leiomodin; Tm, tropomyosin.

enzymes in *I. scapularis* suggested the existence of evolutionarily conserved transcriptional regulation mechanisms in ticks (35). Therefore, to characterize the role of *I. scapularis* tick cytoskeleton components in response to *A. phagocytophilum* infection the mRNA and protein levels of cytoskeleton components were assessed using quantitative transcriptomics and proteomics data (8, 9). The analysis was conducted by comparing uninfected versus *A. phagocytophilum*-infected samples from *I. scapularis* nymphs, adult female midguts and salivary glands, and ISE6 cultured cells that constitute a model for hemocytes (8, 9).

The results showed mRNA/protein-specific and tissue-specific differences between infected and uninfected samples (Figure 2). At the protein level, many proteins were not identified by mass spectrometry, but for the identified proteins the results showed a low (23%) correlation between differential regulation at the mRNA and protein levels (Figure 2). The cytoskeleton components with similar regulation at the mRNA and protein levels included α -tubulin (N=2), β -tubulin (N=4), actin (N=1), septin (N=1), profilin (N=1), lamin (N=1), tropomyosin (N=1), kinesin (N=3), and dynein (N=2) (Figure 2). The α - and β -tubulins showed a variable profile with tissue-specific signatures in response to pathogen infection (Figure 2). Actin regulation at the mRNA and protein levels was similar in nymphs only, and their levels were significantly lower in infected ticks when compared to

uninfected controls (Figure 2). The mRNA and protein levels for Sept1 significantly decreased in response to infection in tick midguts only (Figure 2). In contrast, the levels of all kinesins and dyneins that showed a similar differential regulation at the mRNA and protein levels significantly increased in response to infection in both tick midguts and salivary glands (Figure 2). However, the mRNA and protein levels for two kinesins were significantly lower in infected ISE6 cells when compared to uninfected controls (Figure 2). Regarding actin-related proteins, profilin mRNA and protein levels significantly decreased in both tick midguts and salivary glands, while lamin and tropomyosin levels significantly increased in midguts in response to infection (Figure 2).

As in previous experiments (6), these results supported cytoskeleton remodeling with tissue-specific differences during *A. phagocytophilum* infection in *I. scapularis*.

4.4. Functional studies support a role for cytoskeleton remodeling during *A. phagocytophilum* infection of tick cells

The actin-related protein tropomyosin was selected for functional studies due to its role in the signalling environment to regulate the cytoskeleton (29). Furthermore, tropomyosin protein levels increased in tick midguts and ISE6 cells, and decreased in salivary glands in response to *A. phagocytophilum*

Table 4. Annotation of kinesins and dyneins in the *I. scapularis* genome

Protein family/subunit	Genome accession	GenBank ID	Length (amino acids)
Kinesins			
Kinesin	ISCW008807	EEC12879	717
Kinesin	ISCW019003	EEC08098	700
Kinesin	ISCW006455	EEC07735	301
Kinesin	ISCW013671	EEC18111	379
Kinesin	ISCW014332	EEC18799	247
Kinesin	ISCW014331	EEC18798	535
Kinesin	ISCW011760	EEC15373	173
Kinesin	ISCW020188	EEC11989	245
Kinesin	ISCW011646	EEC14794	565
Kinesin	ISCW020631	EEC13098	706
Dyneins			
Dynein heavy chain	ISCW023533	EEC18129	1310
Dynein heavy chain	ISCW021659	EEC14280	267
Dynein heavy chain	ISCW021660	EEC14281	2827
Dynein heavy chain	ISCW023536	EEC18131	260
Dynein heavy chain	ISCW023535	EEC18130	561
Dynein light chain	ISCW013770	EEC18995	93
Dynein light chain	ISCW022309	EEC16646	106
Dynein light chain	ISCW024736	EEC16583	92
Dynein light chain	ISCW024750	EEC16102	88
Dynein light chain	ISCW021250	EEC14445	109
Dynein light chain	ISCW024480	EEC10091	92
Dynein light chain	ISCW024425	EEC09151	89
Dynein light chain	ISCW018726	EEC08952	304
Dynein light chain	ISCW017907	EEC05270	484
Dynein light chain	ISCW003606	EEC06921	89
Dynein light chain	ISCW011818	EEC14967	115
Dynein light chain	ISCW002098	EEC03087	137
Dynein intermediate chain	ISCW020745	EEC12477	502
Dynein intermediate chain	ISCW016470	EEC00323	413
Dynein intermediate chain	ISCW018553	EEC07157	240

infection (Figure 2). The antibody against tropomyosin used for immunofluorescence recognized the protein in muscle, midguts and salivary glands of *I. scapularis* fed female ticks (Figure 3A). The results of the immunofluorescence assay in *I. scapularis* female ticks validated the proteomics results by showing higher and lower protein levels in tick midguts and salivary glands, respectively in infected ticks when compared to uninfected controls (Figure 3B). A 60% *tropomyosin* silencing was obtained after gene knockdown in tick ISE6 cells when compared to *Rs86* control siRNA-treated cells. The *A. phagocytophilum* DNA levels decreased in tropomyosin siRNA-treated

cells when compared to controls (Figure 3C), supporting an effect of *tropomyosin* knockdown on reducing pathogen infection. Taken together, these results supported a role for cytoskeleton remodeling during *A. phagocytophilum* infection of tick cells.

5. DISCUSSION

Anaplasma phagocytophilum are obligate intracellular pathogens that infect and multiply in both vertebrate and invertebrate tick hosts. These bacteria have one of the smallest genomes (1.47 Mb), and represent a paradigm for reductive evolution (36–38).

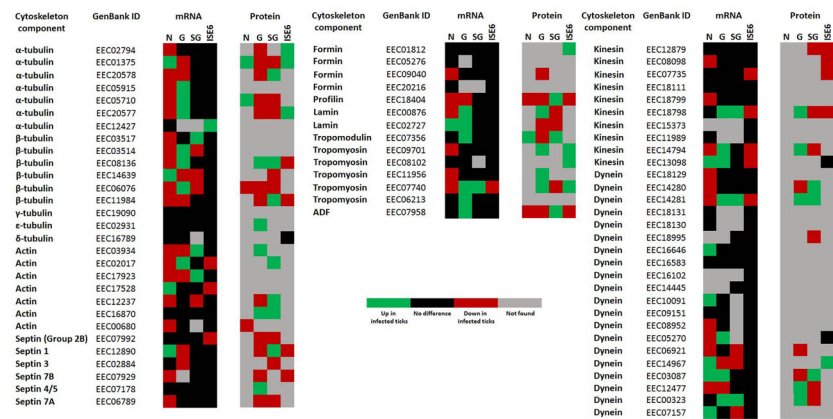


Figure 2. Characterization of the *I. scapularis* cytoskeleton component mRNA and protein levels in response to *A. phagocytophilum* infection. Comparison of cytoskeleton components mRNA and protein levels in *I. scapularis* nymphs (N), female midguts (G), female salivary glands (SG), and ISE6 cells (ISE6) in response to *A. phagocytophilum* infection. Transcriptomics and proteomics data were obtained from previously published datasets, and only statistically significant differences between infected and uninfected samples are shown (8, 9).

Remarkably, *A. phagocytophilum* have a broad host range, and several tick species can act as vectors for these bacteria (3, 39, 40). Therefore, the development of host-specific strategies for infection would have represented a high fitness cost. Instead, recent findings on the molecular characterization of tick-host-pathogen interactions revealed that *A. phagocytophilum* uses common strategies for infection of ticks and vertebrate hosts (4). Among these common strategies is the remodeling of the cytoskeleton (4).

In general, it is widely accepted that intracellular bacteria manipulate the actin cytoskeleton to assist pathogen infection, replication and dissemination (41–43). However, little is known about the function of tick cytoskeleton components during intracellular bacterial infection (43). Here, we found that *I. scapularis* ticks have the same cytoskeleton components described in other organisms such as *H. sapiens*, *D. melanogaster* and *S. cerevisiae*. In human neutrophils, *A. phagocytophilum* infection induces cytoskeleton rearrangement through the regulator of the actomyosin cytoskeleton, ROCK1 (44). Recently, a global proteomics analysis revealed that *A. phagocytophilum* infection changes the protein representation profile of cytoskeleton components in the human promyelocytic leukemia cell line, HL60 (45). In particular, keratin, Arp2/3 protein complex, α -actinin-4, galectin-9, plastin-2 were significantly under-represented, while kinesin-like protein 2 and cofilin were significantly over-represented in HL60 in response to infection (45).

Several components of the *I. scapularis* cytoskeleton such as tubulin, actin, actin-related proteins and motor proteins were differentially expressed/represented in response to *A. phagocytophilum* infection. The role of kinesins and dyneins during the intracellular movement of *Anaplasma* spp.

within host cells remains to be established, but our results suggested that in addition to cytoskeleton rearrangement, motor proteins may play an important role during infection by *A. phagocytophilum* (Figure 4). The rickettsia *Orientia tsutsugamushi*, the causative agent of scrub typhus that also infects vertebrate and invertebrate hosts, uses dynein to propel themselves from the cell periphery to the microtubules organizing center (MTOC) (46). Furthermore, *Chlamydia trachomatis* inclusion membrane protein CT850 interacts with dynein to promote appropriate positioning of the inclusion at the MTOC (47). Additionally, several bacteria such as *Salmonella enterica*, *O. tsutsugamushi*, *Campylobacter jejuni* and *C. trachomatis* use microtubule motor proteins such as kinesins and dyneins for cytoplasmic movement within host cells (46, 48, 49). Notably, kinesin-like proteins were found under-represented and over-represented during *A. phagocytophilum* and *Ehrlichia chaffeensis* infection of HL60 cells, respectively (45). Further research should address whether *A. phagocytophilum* uses host dynein for intracellular movement, and whether dynein-binding proteins that are able to interact with host dynein are encoded in the bacterial genome.

In agreement with our results, Macaluso *et al.* (50) reported that α -tubulin was differentially expressed in response to *Rickettsia montanensis* infection of *Dermacentor variabilis* ticks. They found that the α -tubulin gene was down-regulated in tick midguts, and up-regulated in salivary glands in response to rickettsial infection (50). However, herein we found that the expression of the α -tubulin genes identified in *I. scapularis* did not change significantly in the salivary glands of infected ticks when compared to uninfected controls. The differences in α -tubulin regulation in salivary glands between *R. montanensis* and *A. phagocytophilum* infected ticks may reflect

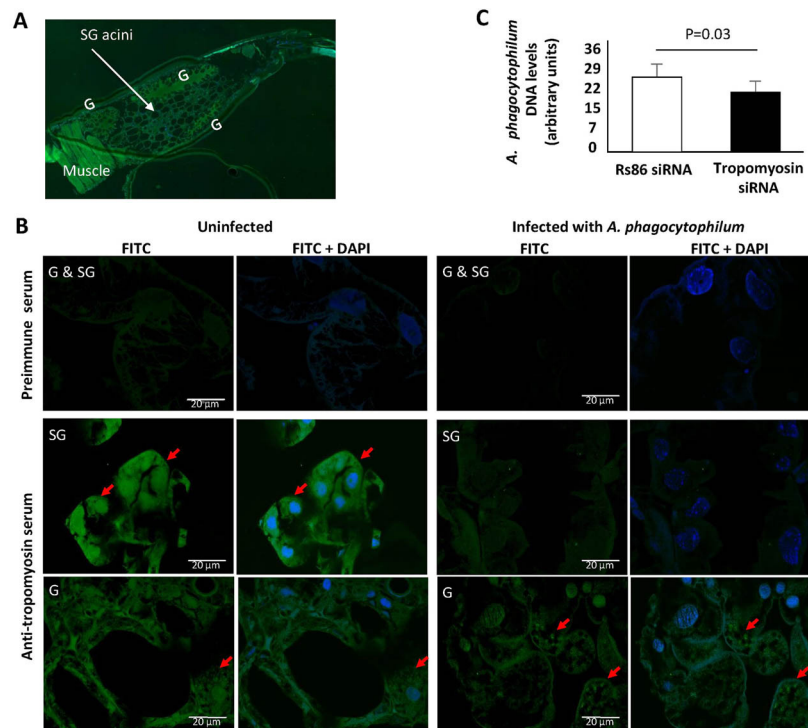


Figure 3. Role of tropomyosin in *A. phagocytophilum* infection of *I. scapularis*. (A) Representative image of a fed *I. scapularis* female tick showing tropomyosin recognition in muscle, midgut (G) and salivary gland (SG) tissues stained with rat anti-tropomyosin monoclonal antibodies (green, FITC) and DAPI (blue). (B) Representative images of immunofluorescence analysis of uninfected and *A. phagocytophilum*-infected adult female *I. scapularis* midguts (G) and salivary glands (SG). Tick tissues were stained with preimmune control serum or rat anti-tropomyosin monoclonal antibodies (green, FITC) or DAPI (blue) and superimposed (FITC+DAPI). Bars, 20 μ m. Red arrows illustrate the positive staining for tropomyosin in tick G and SG. (C) *A. phagocytophilum* DNA levels were determined in infected ISE6 tick cells treated with *tropomyosin* siRNAs or control *Rs86* siRNA, shown as average + S.D., and compared between groups by Student's t-test with unequal variance ($P=0.03$; $N=6$ biological replicates).

pathogen-specific and/or tick-specific responses. However, in agreement with the results of Macaluso *et al.* (50), two of the α -tubulin genes identified in *I. scapularis* were down-regulated, while all α -tubulin proteins were under-represented in midguts in response to infection.

In this study, seven septins were identified in the genome of *I. scapularis*. Septins are recently discovered and important components of eukaryotic cytoskeleton (25). The bacteria *Listeria monocytogenes* and *Shigella flexneri* exploit the host actin cytoskeleton for their own motility and they are attached to long actin tails in the cytosol of the host (51). Septins form a cage around these bacteria-related actin tails, surround bacterial bodies and were suggested to constitute a cellular defense mechanism against pathogens (52, 53). In the case of *Shigella flexneri* (25), septin cages limit bacterial motility and dissemination. The response of tick septins to *A. phagocytophilum* infection was complex. Most septins were down-regulated and under-represented at the mRNA and protein levels, respectively, probably reflecting manipulation of *A. phagocytophilum* to avoid this cellular defense mechanism. However, *I. scapularis* SEPT1 and SEPT4/5 proteins were over-represented

in salivary glands and midguts, respectively, probably reflecting tick response to *A. phagocytophilum* infection (Figure 4). In agreement with these results, different septins seem to have distinct roles during bacterial invasion processes (25).

The decrease in *A. phagocytophilum* infection levels in tick ISE6 cells after *tropomyosin* gene knockdown, suggested that the pathogen remodels tick cytoskeleton, at least in part, by increasing the levels of these actin-related proteins in tick midguts (Figure 4). In tick salivary glands, the decrease in protein representation in response to infection may be associated with tick response to limit pathogen infection. The mechanism by which *A. phagocytophilum* manipulate protein levels in tick cells is unknown, but may include modification of host cell epigenetics by bacterial regulators secreted through the T4 secretion system (T4SS) and other mechanisms (35).

The failure to identify *I. scapularis* orthologs for some genes may be due to the absence of these components in ticks or the fact that only approximately 57% of the genome have been sequenced and assembled for this species (7, 54). These results were

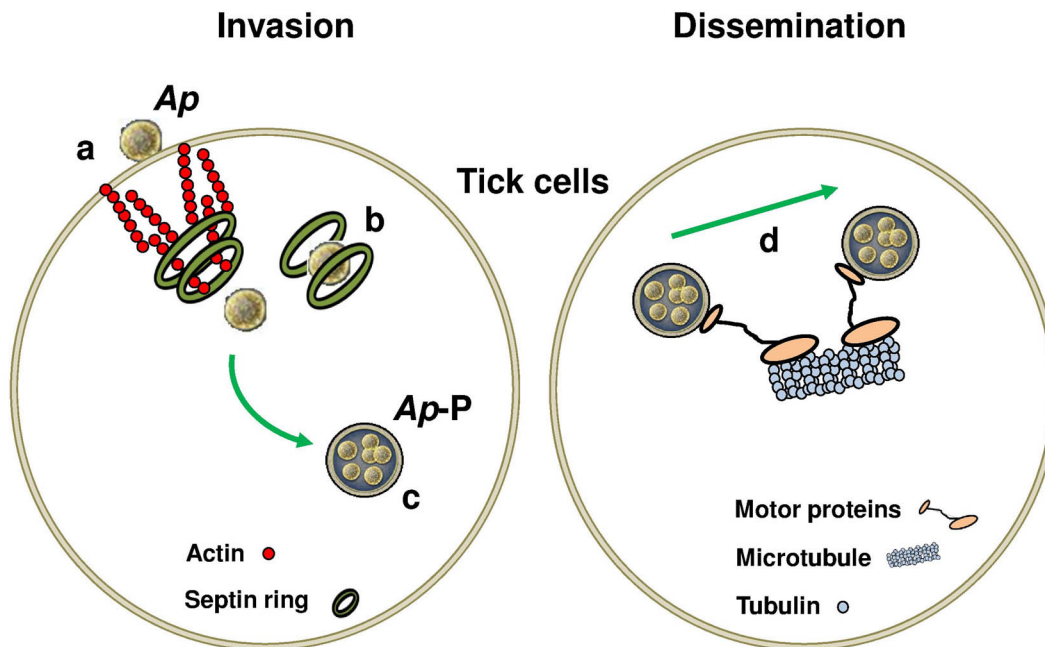


Figure 4. Remodeling of tick cytoskeleton during *A. phagocytophilum* infection. A mechanistic model is proposed by which *A. phagocytophilum* (Ap) induces the production of actins, septins, and actin-related proteins such as tropomyosin, together with actin reorganization to assist tick cell invasion (a). At the same time, infective *A. phagocytophilum* bacteria that fail to form parasitophorous vacuoles (Ap-P; c) will be trapped in septin cages (b). These septin cages (b) may be a mechanism used for tick cells to restrict *A. phagocytophilum* infection. Once parasitophorous vacuoles are formed, tick motor proteins may assist intracytoplasmic movement of *A. phagocytophilum* (d).

similar to those obtained before for other genes and proteins in response to *A. phagocytophilum* infection, showing tissue-specific differences in the response to pathogen infection (8). The transcriptomics and proteomics data of *I. scapularis* nymphs and female midguts and salivary glands in response to *A. phagocytophilum* infection has been validated in several experiments (8, 9, 35). As previously discussed, these results suggested that differences between mRNA and protein levels could be due to delay between mRNA and protein accumulation which requires sampling at different time points and/or the role for post-transcriptional and post-translational modifications in tick tissue-specific response to *A. phagocytophilum* infection (8, 9, 35). In fact, some components of the cytoskeleton are regulated at the transcriptional (55) and translational (56) levels, while other are affected by post-translational modifications (57).

In summary, here we showed that *A. phagocytophilum* remodel tick cytoskeleton for infection (Figure 4). The results showed that tubulin, actin, septin, actin-related proteins and motor proteins were affected by *A. phagocytophilum* infection in *I. scapularis*, and suggested mechanisms by which remodeling of the cytoskeleton assists pathogen infection and dissemination (Figure 4). The present work provides a more comprehensive view of the cytoskeletal components involved in infection and host response to *A.*

phagocytophilum infection in ticks. These results provided additional evidences to support that *A. phagocytophilum* uses similar strategies to infect vertebrate hosts and ticks, including the remodeling of the cytoskeleton.

6. ACKNOWLEDGEMENTS

Alejandro Cabezas-Cruz, and Pilar Alberdi contributed equally to this work. We thank Javier Frontiñán (University of Castilla – La Mancha, UCLM, Spain) and Katherine M. Kocan (Oklahoma State University, OSU, USA) for technical assistance with confocal microscopy. This research was supported by the Ministerio de Economía, Industria y Competitividad (Spain) grant BFU2016–79892-P and the European Union (EU) Seventh Framework Programme (FP7) ANTIGONE project number 278976. MV was supported by the Research Plan of the UCLM. The funders had no role in study design, data collection and interpretation, or the decision to submit the work for publication.

7. REFERENCES

1. J de la Fuente, A Estrada-Peña, J M Venzal, K M Kocan, D E Sonenshine: Overview: Ticks as vectors of pathogens that cause disease in humans and animals. *Front Biosci* 13, 6938–46 (2008)

2. S Stuenkel, E G Granquist, C Silaghi: *Anaplasma phagocytophilum*—a widespread multi-host pathogen with highly adaptive strategies. *Front Cell Infect Microbiol* 3, 31 (2013)
DOI: 10.3389/fcimb.2013.00031
3. K M Kocan, J de la Fuente, A Cabezas-Cruz: The genus *Anaplasma*: new challenges after reclassification. *Rev Sci Tech* 34, 577–86 (2015)
4. J de la Fuente, A Estrada-Peña, A Cabezas-Cruz, K M Kocan: *Anaplasma phagocytophilum* uses common strategies for infection of ticks and vertebrate hosts. *Trends Microbiol* 24, 173–80 (2016)
DOI: 10.1016/j.tim.2015.12.001
5. Y Rikihisa: Mechanisms of obligatory intracellular infection with *Anaplasma phagocytophilum*. *Clin Microbiol Rev* 24, 469–89 (2011)
DOI: 10.1128/CMR.00064–10
6. N Ayllón, M Villar, A T Busby, K M Kocan, E F Blouin, E Bonzón-Kulichenko, R C Galindo, A J Mangold, P Alberdi, J M Pérez de la Lastra, J Vázquez, J de la Fuente: *Anaplasma phagocytophilum* inhibits apoptosis and promotes cytoskeleton rearrangement for infection of tick cells. *Infect Immun* 81, 2415–25 (2013)
DOI: 10.1128/IAI.00194–13
7. M Gulia-Nuss, A B Nuss, J M Meyer, D E Sonenshine, R M Roe, R M Waterhouse, D B Sattelle, J de la Fuente, J M Ribeiro, K Megy, J Thimmapuram, J R Miller, B P Walenz, S Koren, J B Hostetler, M Thiagarajan, V S Joardar, L I Hannick, S Bidwell, M P Hammond, S Young, Q Zeng, J L Abrudan, F C Almeida, N Ayllón, K Bhide, B W Bissinger, E Bonzon-Kulichenko, S D Buckingham, D R Caffrey, M J Caimano, V Croset, T Driscoll, D Gilbert, J J Gillespie, G I Giraldo-Calderón, J M Grabowski, D Jiang, S M Khalil, D Kim, K M Kocan, J Koči, R J Kuhn, T J Kurti, K Lees, E G Lang, R C Kennedy, H Kwon, R Perera, Y Qi, J D Radolf, J M Sakamoto, A Sánchez-Gracia, M S Severo, N Silverman, L Šimo, M Tojo, C Tornador, J P Van Zee, J Vázquez, F G Vieira, M Villar, A R Wespiser, Y Yang, J Zhu, P Arensburger, P V Pietrantonio, S C Barker, R Shao, E M Zdobnov, F Hauser, C J Grimmekhuijzen, Y Park, J Rozas, R Benton, J H Pedra, D R Nelson, M F Unger, J M Tubio, Z Tu, H M Robertson, M Shumway, G Sutton, J R Wortman, D Lawson, S K Wikel, V M Nene, C M Fraser, F H Collins, B Birren, K E Nelson, E Caler, C A Hill: Genomic insights into the *Ixodes scapularis* tick vector of Lyme disease. *Nat Commun* 7, 10507 (2016)
DOI: 10.1038/ncomms10507
8. N Ayllón, M Villar, R C Galindo, K M Kocan, R Šíma, J A López, J Vázquez, P Alberdi, A Cabezas-Cruz, P Kopáček, J de la Fuente: Systems biology of tissue-specific response to *Anaplasma phagocytophilum* reveals differentiated apoptosis in the tick vector *Ixodes scapularis*. *PLoS Genet* 11, e1005120 (2015)
DOI: 10.1371/journal.pgen.1005120
9. M Villar, N Ayllón, P Alberdi, A Moreno, M Moreno, R Tobes, L Mateos-Hernández, S Weisheit, L Bell-Sakyi, J de la Fuente: Integrated metabolomics, transcriptomics and proteomics identifies metabolic pathways affected by *Anaplasma phagocytophilum* infection in tick cells. *Mol Cell Proteomics* 14, 3154–72 (2015)
DOI: 10.1074/mcp.M115.051938
10. S F Altschul, W Gish, W Miller, E W Myers, D J Lipman: Basic local alignment search tool. *J Mol Biol.* 215, 403–10 (1990)
DOI: 10.1016/S0022-2836(05)80360–2
11. T L Madden, R L Tatusov, J Zhang: Applications of network BLAST server. *Methods Enzymol* 266, 131–41 (1996)
12. R D Finn, A Bateman, J Clements, P Coghill, R Y Eberhardt, S R Eddy, A Heger, K Hetherington, L Holm, J Mistry, E L Sonnhammer, J Tate, M Punta: Pfam: the protein families database. *Nucleic Acids Res* 42 (Database issue), D222–30 (2014)
DOI: 10.1093/nar/gkt1223
13. K Katoh, K Kuma, H Toh, T Miyata: MAFFT version 5: improvement in accuracy of multiple sequence alignment. *Nucleic Acids Res* 33, 511–8 (2005)
DOI: 10.1093/nar/gki198
14. K Katoh, D Standley: MAFFT multiple sequence alignment software version 7: improvements in performance and usability. *Mol Biol Evol* 30, 772–80 (2013)
DOI: 10.1093/molbev/mst010
15. J Castresana: Selection of conserved blocks from multiple alignments for their use in phylogenetic analysis. *Mol Biol Evol* 17, 540–52 (2000)

16. D T Jones, W R Taylor, JM Thornton: The rapid generation of mutation data matrices from protein sequences. *CABIOS* 8, 275–282 (1992)
17. K Tamura, G Stecher, D Peterson, A Filipski, S Kumar: MEGA6: Molecular Evolutionary Genetics Analysis version 6.0. *Mol Biol Evol* 30, 2725–9 (2013)
DOI: 10.1093/molbev/mst197
18. U G Munderloh, Y Liu, M Wang, C Chen, T J Kurtti: Establishment, maintenance and description of cell lines from the tick *Ixodes scapularis*. *J Parasitol* 80, 533–43 (1994)
19. K M Asanovich, J S Bakken, J E Madigan, M Aguero-Rosenfeld, G P Wormser, J S Dumler: Antigenic diversity of granulocytic *Ehrlichia* isolates from humans in Wisconsin and New York and a horse in California. *J Infect Dis* 176, 1029–34 (1997)
20. U G Munderloh, S D Jauron, V Fingerle, L Leitritz, S F Hayes, J M Hautman, C M Nelson, B W Huberty, T J Kurtti, G G Ahlstrand, B Greig, M A Mellencamp, J L Goodman: Invasion and intracellular development of the human granulocytic ehrlichiosis agent in tick cell culture. *J Clin Microbiol* 37, 2518–24 (1999)
21. K M Ririe, R P Rasmussen, C T Wittwer: Product differentiation by analysis of DNA melting curves during the polymerase chain reaction. *Anal Biochem* 245, 154–160 (1997)
DOI: 10.1006/abio.1996.9916
22. J Koči, L Šimo, Y Park: Validation of internal reference genes for Real-Time quantitative polymerase chain reaction studies in the tick, *Ixodes scapularis* (Acari: Ixodidae). *J Med Entomol* 50, 79–84 (2013)
23. K J Livak, T D Schmittgen: Analysis of relative gene expression data using real-time quantitative PCR and the 2⁻(Delta Delta C(T)) Method. *Methods* 25, 402–8 (2011)
DOI: 10.1006/meth.2001.1262
24. P W Gunning, U Ghoshdastider, S Whitaker, D Popp, R C Robinson: The evolution of compositionally and functionally distinct actin filaments. *J Cell Sci* 128, 2009–19 (2015)
DOI: 10.1242/jcs.165563
25. S Mostowy, P Cossart: Septins: the fourth component of the cytoskeleton. *Nat Rev Mol Cell Biol* 13, 183–94 (2012)
DOI: 10.1038/nrm3284
26. G M Cooper: The Cell: A Molecular Approach, 2nd Edition. Eds: Sinauer Associates, Sunderland, Massachusetts (2000)
27. F Pan, R L Malmberg, M Momany: Analysis of septins across kingdoms reveals orthology and new motifs. *BMC Evol Biol* 7, 103 (2007)
DOI: 10.1186/1471–2148-7–103
28. S Yamashiro, D S Gokhin, S Kimura, R B Nowak, V M Fowler: Tropomodulins: pointed-end capping proteins that regulate actin filament architecture in diverse cell types. *Cytoskeleton* 69, 337–70 (2012)
DOI: 10.1002/cm.21031
29. G M O'Neill, J Stehn, P W Gunning: Tropomyosins as interpreters of the signalling environment to regulate the local cytoskeleton. *Semin Cancer Biol* 18, 35–44 (2008)
DOI: 10.1016/j.semcancer.2007.08.004
30. J A Theriot, T J Mitchison: The three faces of profilin. *Cell* 75, 835–8 (1993)
31. B L Goode, M J Eck: Mechanism and function of formins in the control of actin assembly. *Annu Rev Biochem* 76, 593–627 (2007)
DOI: 10.1146/annurev.biochem.75.103004.142647
32. E M Roy-Zokan, K A Dyer, R B Meagher: Phylogenetic patterns of codon evolution in the actin-depolymerizing factor/cofilin (ADF/CFL) gene family. *PLoS One* 10, e0145917 (2015)
DOI: 10.1371/journal.pone.0145917
33. L Hering, J E Bouameur, J Reichelt, T M Magin, G Mayer: Novel origin of lamin-derived cytoplasmic intermediate filaments in tardigrades. *Elife* 5, e11117 (2016)
DOI: 10.7554/eLife.11117
34. J C Adam, J R Pringle, M Peifer: Evidence for functional differentiation among *Drosophila* septins in cytokinesis and cellularization. *Mol Biol Cell* 11, 3123–35 (2000)
35. A Cabezas-Cruz, P Alberdi, N Ayllón, J J Valdés, R Pierce, M Villar, J de la Fuente: *Anaplasma phagocytophilum* increases

- the levels of histone modifying enzymes to inhibit cell apoptosis and facilitate pathogen infection in the tick vector *Ixodes scapularis*. *Epigenetics* 11, 303–19 (2016)
DOI: 10.1080/15592294.2016.1163460
36. H J C Dunning, M Lin, R Madupu, J Crabtree, S V Angiuoli, J A Eisen, R Seshadri, Q Ren, M Wu, T R Utterback, S Smith, M Lewis, H Khouri, C Zhang, H Niu, Q Lin, N Ohashi, N Zhi, W Nelson, L M Brinkac, R J Dodson, M J Rosovitz, J Sundaram, S C Daugherty, T Davidsen, A S Durkin, M Gwinn, D H Haft, J D Selengut, S A Sullivan, N Zafar, L Zhou, F Benahmed, H Forberger, R Halpin, S Mulligan, J Robinson, O White, Y Rikihisa, H Tettelin: Comparative genomics of emerging human ehrlichiosis agents. *PLoS Genet* 2, e21 (2006)
DOI: 10.1371/journal.pgen.0020021
37. G Blanc, H Ogata, C Robert, S Audic, K Suhre, G Vestris, J M Claverie, D Raoult: Reductive genome evolution from the mother of *Rickettsia*. *PLoS Genet* 3, e14 (2007)
DOI: 10.1371/journal.pgen.0030014
38. A C Darby, N H Cho, H H Fuxelius, J Westberg, S G Andersson: Intracellular pathogens go extreme: genome evolution in the Rickettsiales. *Trends Genet* 23, 511–20 (2007)
DOI: 10.1016/j.tig.2007.08.002
39. J de la Fuente, A Estrada-Peña, A Cabezas-Cruz, R Brey: Flying ticks: anciently evolved associations that constitute a risk of infectious disease spread. *Parasit Vectors* 8, 538 (2015)
DOI: 10.1186/s13071-015-1154-1
40. A Estrada-Peña, J de la Fuente, R S Ostfeld, A Cabezas-Cruz: Interactions between tick and transmitted pathogens evolved to minimise competition through nested and coherent networks. *Sci Rep* 5, 10361 (2015)
DOI: 10.1038/srep10361
41. P Cossart, P J Sansonetti: Bacterial invasion: the paradigms of enteroinvasive pathogens. *Science* 304, 242–8 (2004)
DOI: 10.1126/science.1090124
42. C M Haglund, M D Welch: Pathogens and polymers: microbe-host interactions illuminate the cytoskeleton. *J Cell Biol* 195, 7–17 (2011)
DOI: 10.1083/jcb.201103148
43. P M Colonne, C G Winchell, D E Voth: Hijacking host cell highways: manipulation of the host actin cytoskeleton by obligate intracellular bacterial pathogens. *Front Cell Infect Microbiol* 6, 107 (2016)
DOI: 10.3389/fcimb.2016.00107
44. V Thomas, E Fikrig: *Anaplasma phagocytophilum* specifically induces tyrosine phosphorylation of ROCK1 during infection. *Cell Microbiol* 9, 1730–7 (2007)
DOI: 10.1111/j.1462-5822.2007.00908.x
45. M Lin, T Kikuchi, H M Brewer, A D Norbeck, Y Rikihisa: Global proteomic analysis of two tick-borne emerging zoonotic agents: *Anaplasma phagocytophilum* and *Ehrlichia chaffeensis*. *Front Microbiol* 2, 24 (2011)
DOI: 10.3389/fmicb.2011.00024
46. S W Kim, K S Ihn, S H Han, S Y Seong, I S Kim, M S Choi: Microtubule- and dynein-mediated movement of *Orientia tsutsugamushi* to the microtubule organizing center. *Infect Immun* 69, 494–500 (2001)
DOI: 10.1128/IAI.69.1.494-500.2001
47. J Mital, E I Lutter, A C Barger, C A Dooley, T Hackstadt: *Chlamydia trachomatis* inclusion membrane protein CT850 interacts with the dynein light chain DYNLT1 (Tctex1). *Biochem Biophys Res Commun* 462, 165–70 (2015)
DOI: 10.1016/j.bbrc.2015.04.116
48. L Hu, D J Kopecko: *Campylobacter jejuni* 81–176 associates with microtubules and dynein during invasion of human intestinal cells. *Infect Immun* 67, 4171–82 (1999)
49. A E Ramsden, L J Mota, S Mütter, S L Shorte, D W Holden: The SPI-2 type III secretion system restricts motility of *Salmonella*-containing vacuoles. *Cell Microbiol* 9, 2517–29 (2007)
DOI: 10.1111/j.1462-5822.2007.00977.x
50. K R Macaluso, A Mulenga, J A Simser, A F Azad: Differential expression of genes in uninfected and rickettsia-infected *Dermacentor variabilis* ticks as assessed by differential-display PCR. *Infect Immun* 71, 6165–70 (2003)
51. M D Welch, M Way: Arp2/3-mediated actin-based motility: a tail of pathogen abuse. *Cell Host Microbe* 14, 242–55 (2013)
DOI: 10.1016/j.chom.2013.08.011

52. M Kinoshita, C M Field, M L Coughlin, A F Straight, T J Mitchison: Self- and actin-templated assembly of Mammalian septins. *Dev Cell* 3, 791–802 (2002)
53. S Mostowy, M Bonazzi, M A Hamon, T N Tham, A Mallet, M Lelek, E Gouin, C Demangel, R Brosch, C Zimmer, A Sartori, M Kinoshita, M Lecuit, P Cossart: Entrapment of intracytosolic bacteria by septin cage-like structures. *Cell Host Microbe* 8, 433–44 (2010)
DOI: 10.1016/j.chom.2010.10.009
54. J de la Fuente, R M Waterhouse, D E Sonenshine, R Roe, J Ribeiro, D B Sattelle, C A Hill: Tick genome assembled: new opportunities for research on tick-host-pathogen interactions. *Front Cell Infect Microbiol* 6, 103 (2016)
DOI: 10.3389/fcimb.2016.00103
55. T Morita, T Mayanagi, K Sobue: Reorganization of the actin cytoskeleton via transcriptional regulation of cytoskeletal/focal adhesion genes by myocardin-related transcription factors (MRTFs/MAL/MKLs). *Exp Cell Res* 313, 3432–45 (2007)
DOI: 10.1016/j.yexcr.2007.07.008
56. S F Gilbert. *Developmental Biology*, 6th edition. Eds: Sinauer Associates, Sunderland, Massachusetts (2000)
57. Y Song, S T Brady: Post-translational modifications of tubulin: pathways to functional diversity of microtubules. *Trends Cell Biol* 25, 125–36 (2015)
DOI: 10.1016/j.tcb.2014.10.004

Key Words: Cytoskeleton, Proteomics, Transcriptomics, *Ixodes scapularis*, *Anaplasma phagocytophilum*

Send correspondence to: Jose de la Fuente, SaBio Instituto de Investigacion en Recursos Cinegeticos IREC (CSIC-UCLM-JCCM), 13005 Ciudad Real, Spain, Tel: 34-926295450, Fax: 34-926295451, E-mail: jose_delafuente@yahoo.com